

## Article

# Elevated CO<sub>2</sub> Concentration Alters Photosynthetic Performances under Fluctuating Light in *Arabidopsis thaliana*

Shun-Ling Tan <sup>1,2</sup>, Xing Huang <sup>1</sup>, Wei-Qi Li <sup>1</sup> , Shi-Bao Zhang <sup>1,\*</sup> and Wei Huang <sup>1,\*</sup> 

<sup>1</sup> Kunming Institute of Botany, Chinese Academy of Sciences, Kunming 650201, China; tanshunling@mail.kib.ac.cn (S.-L.T.); huangxing@mail.kib.ac.cn (X.H.); weiqili@mail.kib.ac.cn (W.-Q.L.)

<sup>2</sup> University of Chinese Academy of Sciences, Beijing 100049, China

\* Correspondence: sbzhang@mail.kib.ac.cn (S.-B.Z.); huangwei@mail.kib.ac.cn (W.H.)

**Abstract:** In view of the current and expected future rise in atmospheric CO<sub>2</sub> concentrations, we examined the effect of elevated CO<sub>2</sub> on photoinhibition of photosystem I (PSI) under fluctuating light in *Arabidopsis thaliana*. At 400 ppm CO<sub>2</sub>, PSI showed a transient over-reduction within the first 30 s after transition from dark to actinic light. Under the same CO<sub>2</sub> conditions, PSI was highly reduced after a transition from low to high light for 20 s. However, such PSI over-reduction greatly decreased when measured in 800 ppm CO<sub>2</sub>, indicating that elevated atmospheric CO<sub>2</sub> facilitates the rapid oxidation of PSI under fluctuating light. Furthermore, after fluctuating light treatment, residual PSI activity was significantly higher in 800 ppm CO<sub>2</sub> than in 400 ppm CO<sub>2</sub>, suggesting that elevated atmospheric CO<sub>2</sub> mitigates PSI photoinhibition under fluctuating light. We further demonstrate that elevated CO<sub>2</sub> does not affect PSI activity under fluctuating light via changes in non-photochemical quenching or cyclic electron transport, but rather from a rapid electron sink driven by CO<sub>2</sub> fixation. Therefore, elevated CO<sub>2</sub> mitigates PSI photoinhibition under fluctuating light at the acceptor rather than the donor side. Taken together, these observations indicate that elevated atmospheric CO<sub>2</sub> can have large effects on thylakoid reactions under fluctuating light.

**Keywords:** CO<sub>2</sub> concentration; photosynthesis; photosystem I; redox state of P700



**Citation:** Tan, S.-L.; Huang, X.; Li, W.-Q.; Zhang, S.-B.; Huang, W. Elevated CO<sub>2</sub> Concentration Alters Photosynthetic Performances under Fluctuating Light in *Arabidopsis thaliana*. *Cells* **2021**, *10*, 2329.

<https://doi.org/10.3390/cells10092329>

Academic Editor: Hazem M. Kalaji

Received: 3 August 2021

Accepted: 20 August 2021

Published: 6 September 2021

**Publisher's Note:** MDPI stays neutral with regard to jurisdictional claims in published maps and institutional affiliations.



**Copyright:** © 2021 by the authors. Licensee MDPI, Basel, Switzerland. This article is an open access article distributed under the terms and conditions of the Creative Commons Attribution (CC BY) license (<https://creativecommons.org/licenses/by/4.0/>).

## 1. Introduction

Photosynthetic organisms absorb light energy to drive photosynthetic electron flow and CO<sub>2</sub> assimilation. In linear electron flow (LEF), electrons are transferred from photosystem II (PSII) to photosystem I (PSI), and ultimately to NADP<sup>+</sup>, producing NADPH. This electron flow is coupled to the formation of proton motive force that powers the regeneration of ATP. In cyclic electron flow (CEF) around PSI, electrons are transported from ferredoxin into the plastoquinone pool, generating ATP without producing NADPH. PSI and PSII work co-operatively to form ATP and NADPH, which is essential for the primary metabolism. Once PSII is photoinhibited, as indicated by the decrease in the maximum quantum yield of PSII ( $F_v/F_m$ ), LEF would be suppressed [1]. Once PSI is photodamaged, as indicated by the decrease in the maximum photo-oxidizable P700 ( $P_m$ ), both LEF and CEF are depressed, which will affect CO<sub>2</sub> fixation and impair plant growth [2–6].

Photosynthetic organisms are often exposed to dynamic fluctuations in light intensity when grown in the field [7–9]. Under such fluctuating light (FL) conditions, an abrupt increase in light intensity will lead to an immediate rise in light absorption, triggering electron flow from PSII to PSI [10–12]. Meanwhile, CO<sub>2</sub> assimilation has a much slower kinetics than electron flow from PSII [7,13,14]. Therefore, NADPH cannot be immediately consumed by CO<sub>2</sub> assimilation. Because the pool size of NADPH is relatively small, such an imbalance between electron flow and primary metabolism leads to an increase in the NADPH/NADP<sup>+</sup> ratio. The lack of NADP<sup>+</sup> restricts LEF and thus induces the accumulation of excited states at PSI, resulting in the generation of reactive oxygen species

(ROS) in PSI [15,16]. Because the ROS produced in PSI cannot be immediately scavenged by antioxidant system [17], FL can cause selective photodamage to PSI [16,18,19].

Accordingly, photosynthetic organisms employ several alternative electron transport routes to protect PSI under FL [20–22]. In *Arabidopsis* (*A. thaliana*), the *proton gradient regulation 5* (*pgr5*) is seedling-lethal when grown under FL, as a consequence of uncontrolled PSI photoinhibition due to a defect in CEF [23]. Therefore, CEF is essential for PSI photoprotection under FL in angiosperms [16,24,25]. During CEF, electrons from ferredoxin are transferred to plastoquinone, generating a  $\Delta\text{pH}$  without reducing  $\text{NADP}^+$  [24,26–28]. In response to a sudden increase in irradiance, CEF first rises before gradually decreasing and reaching a constant rate [29–32]. The initial stimulation of CEF facilitates the rapid formation of  $\Delta\text{pH}$  [29], slowing down the electron flow at the cytochrome (Cyt)  $b_6/f$  complex and increasing the ATP/NADPH production ratio [33,34]. CEF therefore protects PSI under FL at both electron donor and acceptor sides [16]. Once  $\Delta\text{pH}$  reaches a sufficient level, CEF activity decreases to a steady state to avoid over-acidification of the thylakoid lumen, thus optimizing the tradeoff between photosynthesis and photoprotection [29,35]. Therefore, CEF plasticity plays an important role in sustaining photosynthesis under FL.

One of the main drivers of global climate change, atmospheric  $\text{CO}_2$  concentrations are expected to continue increasing in the near future. Higher atmospheric  $\text{CO}_2$  may lead to a rise in intercellular and chloroplast  $\text{CO}_2$  concentrations, which will boost the rate of  $\text{CO}_2$  assimilation and plant growth [36,37]. However, the maintenance of a high level of PSI activity is essential for optimal photosynthesis. Once PSI photoinhibition occurs under FL, the rate of  $\text{CO}_2$  assimilation under higher atmospheric  $\text{CO}_2$  conditions will also suffer [3]. Therefore, the predicted positive effects of elevated atmospheric  $\text{CO}_2$  on crop yield are not only a reflection of the rate of  $\text{CO}_2$  fixation, but are also likely linked to light reactions. However, how elevated atmospheric  $\text{CO}_2$  affects light reactions under FL is largely known.

Theoretically, an elevated concentration of atmospheric  $\text{CO}_2$  will raise the photosynthetic induction rate when transitioning to high light [38,39], increasing the NADPH consumption rate and leading to an increase in the  $\text{NADP}^+/\text{NADPH}$  ratio. Consequently, elevated atmospheric  $\text{CO}_2$  concentrations might facilitate electron flow from PSI to  $\text{NADP}^+$ , with the potential to alleviate the over-reduction of PSI under FL. However, it is unclear whether elevated atmospheric  $\text{CO}_2$  will in fact break the imbalance between light and dark reactions of photosynthesis and alleviate PSI photoinhibition under FL. In the present study, we measured the chlorophyll fluorescence and PSI signals under FL at 400 and 800 ppm  $\text{CO}_2$  concentrations in *Arabidopsis* leaves. The aims of this study were to (1) assess the effect of elevated  $\text{CO}_2$  on the redox state of PSI under FL and (2) examine whether elevated  $\text{CO}_2$  can mitigate PSI photoinhibition under FL.

## 2. Materials and Methods

### 2.1. Plant Materials

*Arabidopsis* (*Arabidopsis thaliana*) wild-type plants grown in a greenhouse (light intensity  $\sim 100 \mu\text{mol photons m}^{-2} \text{s}^{-1}$ , 12-h photoperiod, 25 °C, 60% humidity, 400 ppm  $\text{CO}_2$ ) for 6–8 weeks after germination. We used fully expanded but not senescent leaves for photosynthetic measurements.

### 2.2. Measurement of P700 Redox Kinetics

After incubation in darkness for 60 min, we used a Dual-PAM 100 measuring system (Heinz Walz, Effeltrich, Germany) to record the P700 redox kinetics following the transition from darkness to a light intensity of  $1809 \mu\text{mol photons m}^{-2} \text{s}^{-1}$  for 20 s at 400 or 800 ppm  $\text{CO}_2$ . All photosynthetic measurements were conducted in a phytotron. The air temperature was set to 25 °C; the relative humidity was set to 60%; the  $\text{CO}_2$  concentrations were set to 60% and 400 or 800 ppm.

### 2.3. PSI and PSII Measurements

After dark adaptation for 15 min, plants were illuminated at  $272 \mu\text{mol photons m}^{-2} \text{s}^{-1}$  for 10 min to activate photosynthesis. Afterward, plants were exposed to FL alternating between LL ( $59 \mu\text{mol photons m}^{-2} \text{s}^{-1}$ ) and HL ( $1809 \mu\text{mol photons m}^{-2} \text{s}^{-1}$ ), and the changes in PSI and PSII parameters were recorded using a Dual-PAM 100 measuring system. The quantum yield of PSI photochemistry ( $Y(\text{I})$ ), the quantum yield of PSI non-photochemical energy dissipation due to donor side limitation ( $Y(\text{ND})$ ), and the quantum yield of non-photochemical energy dissipation due to acceptor side limitation ( $Y(\text{NA})$ ) were calculated with the following formulas [40]:  $Y(\text{I}) = (P_m' - P)/P_m$ ,  $Y(\text{ND}) = P/P_m$  and  $Y(\text{NA}) = (P_m - P_m')/P_m$ .

The PSII parameters were calculated with another three formulas [41,42]:  $Y(\text{II}) = (F_m' - F_s)/F_m'$ ,  $Y(\text{NO}) = F_s/F_m$  and  $\text{NPQ} = (F_m - F_m')/F_m'$ .  $Y(\text{II})$  was the effective quantum yield;  $Y(\text{NO})$  was the quantum yield of non-regulated energy dissipation in PSII; NPQ was the non-photochemical quenching in PSII.  $F_s$  was the steady state after light adaptation.  $F_m$  and  $F_m'$  represented the maximum fluorescence after dark and light adaptation, respectively.  $F_m$  was measured after dark-adaptation for 15 min. The photosynthetic electron transport rate through PSI (or PSII) was calculated as:  $\text{ETRI}$  (or  $\text{ETR}_{\text{II}}$ ) =  $\text{PPFD} \times Y(\text{I})$  (or  $Y(\text{II})$ )  $\times 0.84 \times 0.5$ , where PPFD is the photosynthetic photon flux density, and the light absorption of incident irradiance is assumed to be 0.84.

### 2.4. Statistical Analysis

All results are displayed as mean values of five individual experiments.  $t$ -tests were used to determine the significant differences between different treatments ( $\alpha = 0.05$ ).

## 3. Results

### 3.1. Elevated Atmospheric $\text{CO}_2$ Affects the PSI Redox State after Transition from Dark to Light

After transition from darkness to  $1809 \mu\text{mol photons m}^{-2} \text{s}^{-1}$ , P700 became gradually re-oxidized in 20 s when measured in 800 ppm  $\text{CO}_2$  (Figure 1). However, we failed to observe a similar re-oxidation of P700 in 400 ppm  $\text{CO}_2$  (Figure 1). The rapid re-oxidation of P700 after transition from darkness to light is attributed to the outflow of electrons from PSI to downstream electron acceptors [43–45]. Because photo-reduction of  $\text{O}_2$  mediated by flavodiiron proteins and water–water cycle are not observed in *A. thaliana*, the difference in P700 redox kinetics between 400 and 800 ppm  $\text{CO}_2$  suggested that elevated atmospheric  $\text{CO}_2$  accelerates the outflow of electrons from PSI to  $\text{NADP}^+$ , probably due to the increased rate of  $\text{CO}_2$  fixation.

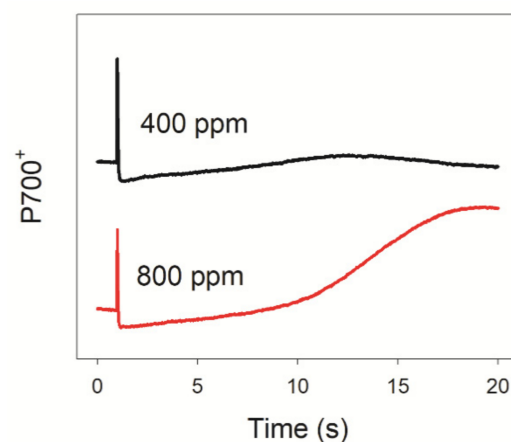


**Figure 1.** Changes in P700 redox kinetics after transition from darkness to actinic light ( $1809 \mu\text{mol photons m}^{-2} \text{s}^{-1}$ ) in 400 and 800 ppm atmospheric  $\text{CO}_2$ . Data are shown as mean values of five leaves from five individual plants.

During photosynthetic induction at a moderate light of  $272 \mu\text{mol photons m}^{-2} \text{s}^{-1}$ , the quantum yield of PSI photochemistry ( $Y(\text{I})$ ) was enhanced at 800 ppm  $\text{CO}_2$  (Figure 2A). The quantum yield of PSI non-photochemical energy dissipation due to the donor side limitation ( $Y(\text{ND})$ ) remained at a low level for 30 s upon transfer from dark to light when measured in 400 ppm  $\text{CO}_2$  (Figure 2B). This led to the over-reduction of PSI, as indicated by the high value of PSI acceptor side limitation ( $Y(\text{NA})$ ) at the same time point (Figure 2C). By comparison,  $Y(\text{ND})$  had already almost reached its maximal value within 30 s in 800 ppm  $\text{CO}_2$  (Figure 2B), resulting in a correspondingly low  $Y(\text{NA})$  value (Figure 2C). Therefore, elevated atmospheric  $\text{CO}_2$  concentrations significantly affected the redox state of PSI during transition from darkness to actinic light. By contrast, elevated atmospheric  $\text{CO}_2$  had minor effects on electron flow from PSII (ETR<sub>II</sub>) and non-photochemical quenching (NPQ) within the first 30 s after transition from darkness to light (Figure 2D,E). Thus, we concluded that the effects of elevated  $\text{CO}_2$  concentration on PSI redox state are not caused by electron flow from PSII or the formation of a  $\Delta\text{pH}$ . Instead, an increase in  $\text{CO}_2$  concentration raises the rate of  $\text{CO}_2$  fixation and thus facilitates electron transfer from PSI to  $\text{NADP}^+$ , which in turn alleviates the over-reduction of PSI.

### 3.2. Elevated Atmospheric $\text{CO}_2$ Affect PSI and PSII Performances Differently after Transition from LL to HL

Next, we examined the effect of elevated atmospheric  $\text{CO}_2$  on photosynthetic performances after transition from LL ( $59 \mu\text{mol photons m}^{-2} \text{s}^{-1}$ ) to HL ( $1809 \mu\text{mol photons m}^{-2} \text{s}^{-1}$ ). The value of quantum yield of PSI photochemistry ( $Y(\text{I})$ ) under LL was slightly higher in 800 ppm  $\text{CO}_2$  than in 400 ppm  $\text{CO}_2$  (Figure 3A). After transition from LL to HL,  $Y(\text{I})$  did not differ between 400 and 800 ppm  $\text{CO}_2$  (Figure 3A). However, within the first 10 s after transition from LL to HL,  $Y(\text{ND})$  was significantly higher in 800 ppm  $\text{CO}_2$  than in 400 ppm  $\text{CO}_2$  (Figure 3B). This rapid oxidation of PSI in 800 ppm  $\text{CO}_2$  alleviated the over-reduction of PSI electron carriers under FL (Figure 3C). In contrast to PSI, PSII performance under FL did not change significantly as a function of atmospheric  $\text{CO}_2$  concentration (Figure 4). Indeed, the effective quantum yield of PSII,  $Y(\text{II})$ , first decreased and then gradually rose upon a sudden transition from LL to HL, as expected (Figure 4A). Meanwhile, NPQ rapidly increased upon transfer to HL (Figure 4B), suggesting the gradual formation of a  $\Delta\text{pH}$ . After transition from LL to HL, the quantum yield of non-regulatory energy dissipation in PSII ( $Y(\text{NO})$ ) increased sharply before undergoing a rapid drop (Figure 4C). Furthermore, the redox state of the plastoquinone pool of PSII ( $q\text{P}$ ) did not differ significantly between 400 and 800 ppm (Figure 4D).

At LL, the ETR<sub>I</sub>/ETR<sub>II</sub> ratio was close to 1 when measured at 400 and 800 ppm (Figure 5A). Within the first 10 s after the transition from LL to HL, the ETR<sub>I</sub>/ETR<sub>II</sub> ratio was very high in exposed leaves (Figure 5A). Such an increase in the ETR<sub>I</sub>/ETR<sub>II</sub> ratio indicated that CEF was stimulated after transition to HL. Furthermore, we noticed that the change in ETR<sub>I</sub>/ETR<sub>II</sub> ratio under FL largely correlated with the PSI acceptor side limitation (Figure 5B). Once PSI was over-reduced, CEF was stimulated to help the rapid formation of  $\Delta\text{pH}$ . Once the over-reduction of PSI has been relaxed, CEF activity decreased to the steady state. Therefore, CEF plays an important role in the regulation of photosynthetic rates under fluctuating light.

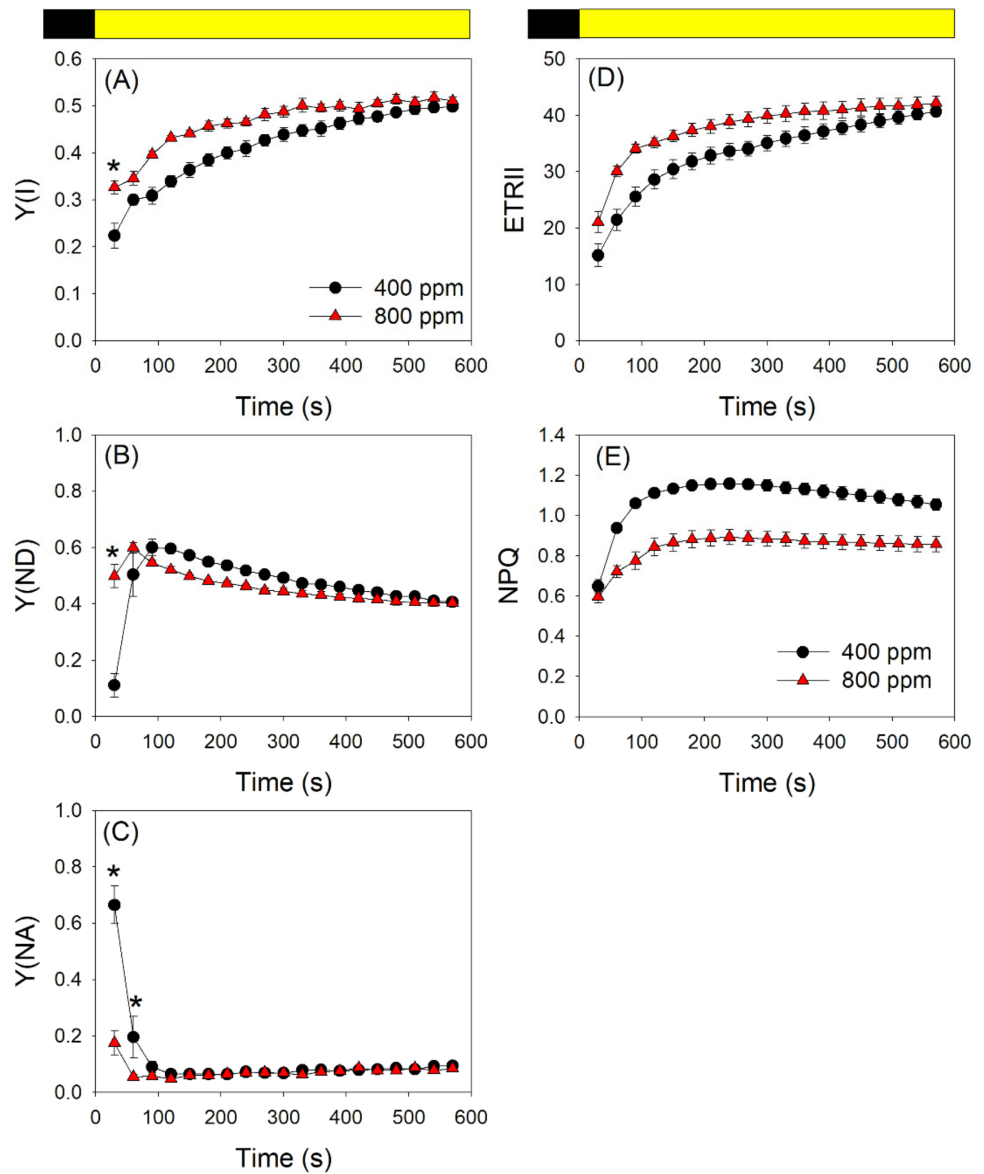


**Figure 2.** Changes in PSI and PSII parameters after transition from darkness to  $272 \mu\text{mol photons m}^{-2} \text{s}^{-1}$  in Arabidopsis leaves, measured in 400 and 800 ppm  $\text{CO}_2$ . (A) Y(I), the quantum yield of PSI photochemistry; (B) Y(ND), the quantum yield of PSI non-photochemical energy dissipation due to the donor side limitation; (C) Y(NA), the quantum yield of PSI non-photochemical energy dissipation due to the acceptor side limitation; (D) ETRII, electron transport rate through PSII; (E) NPQ, non-photochemical quenching in PSII. Data are shown as means  $\pm$  SD ( $n = 5$ ). Asterisk indicates a significant different between 400 and 800 ppm.

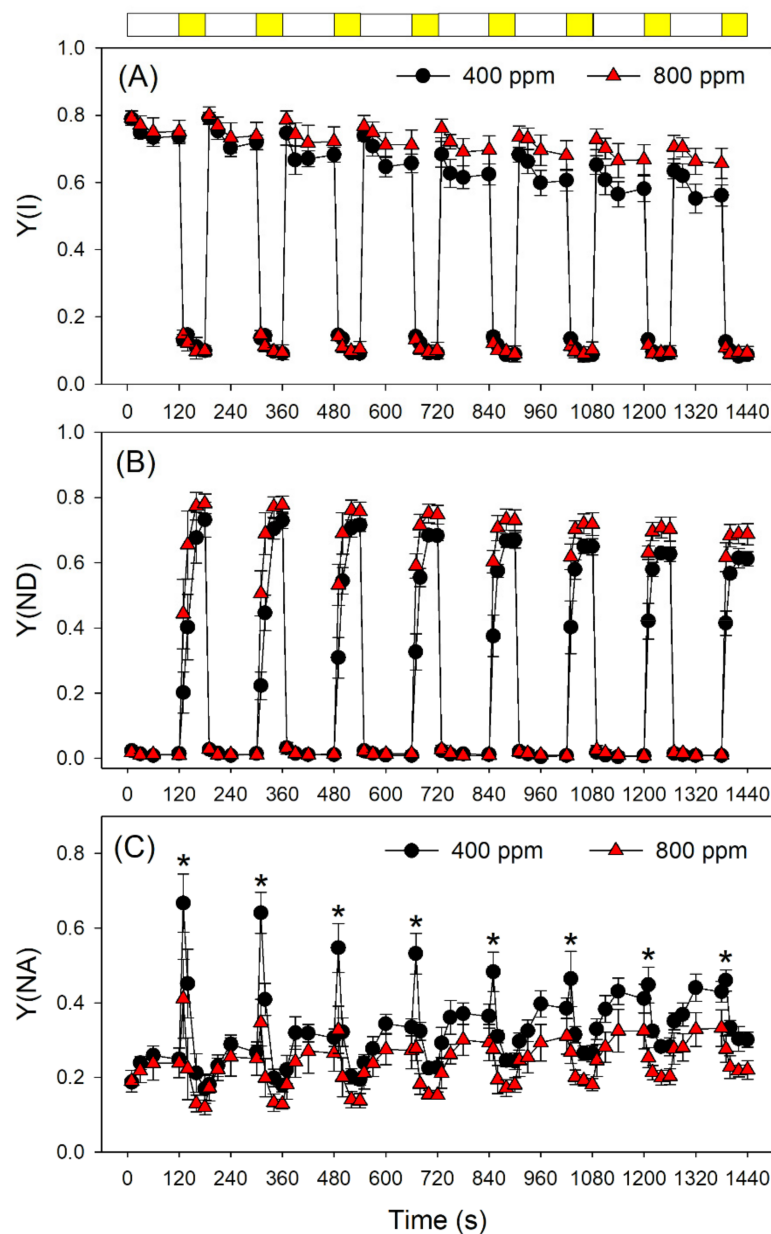


**Figure 3.** Changes in PSI parameters during fluctuating light alternating between 59 and 1809  $\mu\text{mol photons m}^{-2} \text{s}^{-1}$  in Arabidopsis leaves, measured in 400 and 800 ppm CO<sub>2</sub>. (A) Y(I), the quantum yield of PSI photochemistry; (B) Y(ND), the quantum yield of PSI non-photochemical energy dissipation due to the donor side limitation; (C) Y(NA), the quantum yield of PSI non-photochemical energy dissipation due to the acceptor side limitation. Data are shown as means  $\pm$  SD ( $n = 5$ ). White bars indicate low light ( $59 \mu\text{mol photons m}^{-2} \text{s}^{-1}$ ); yellow bars indicate high light ( $1809 \mu\text{mol photons m}^{-2} \text{s}^{-1}$ ). Asterisk indicates a significant difference between 400 and 800 ppm.

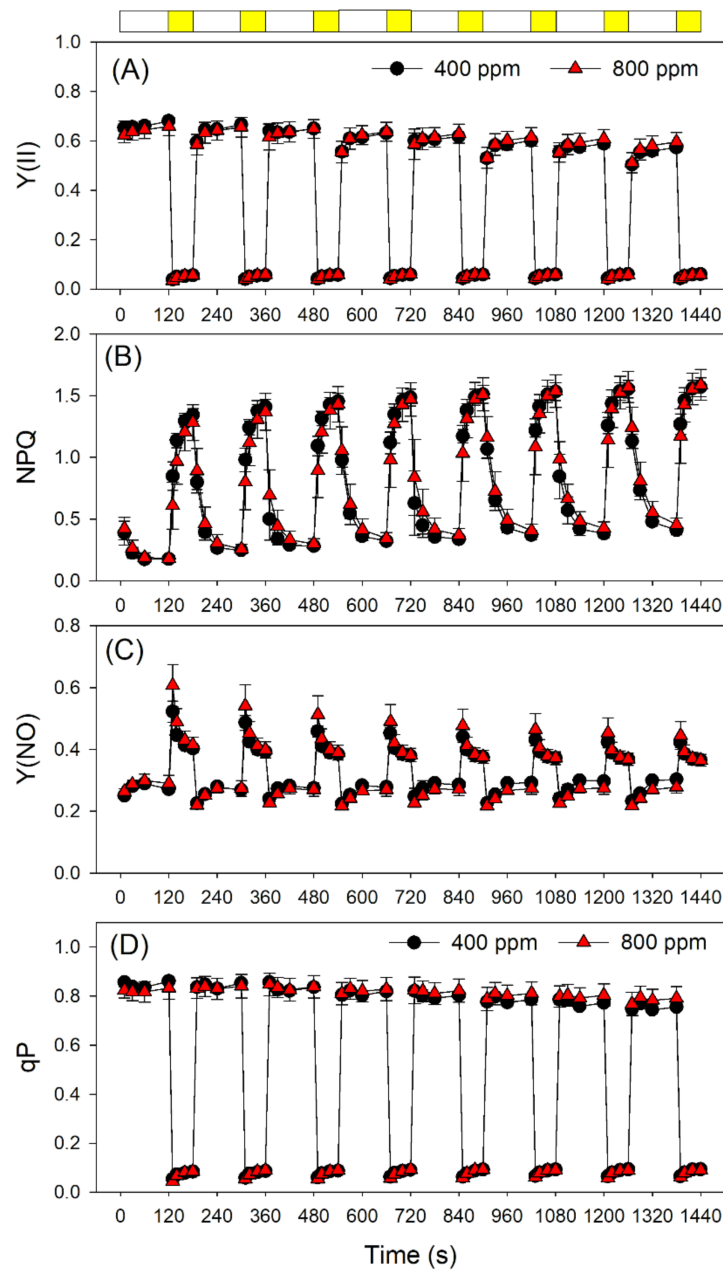


**Figure 4.** Changes in PSII parameters during fluctuating light alternating between 59 and 1809  $\mu\text{mol photons m}^{-2} \text{s}^{-1}$  in Arabidopsis leaves measured in 400 and 800 ppm  $\text{CO}_2$ . **(A)** Y(II), the effective quantum yield of PSII photochemistry; **(B)** NPQ, non-photochemical quenching in PSII; **(C)** Y(NO), the quantum yield of non-regulatory energy dissipation in PSII; **(D)** the redox state of the plastoquinone pool of PSII (qP). Data are shown as means  $\pm$  SD ( $n = 5$ ). White bars indicate low light ( $59 \mu\text{mol photons m}^{-2} \text{s}^{-1}$ ); yellow bars indicate high light ( $1809 \mu\text{mol photons m}^{-2} \text{s}^{-1}$ ).

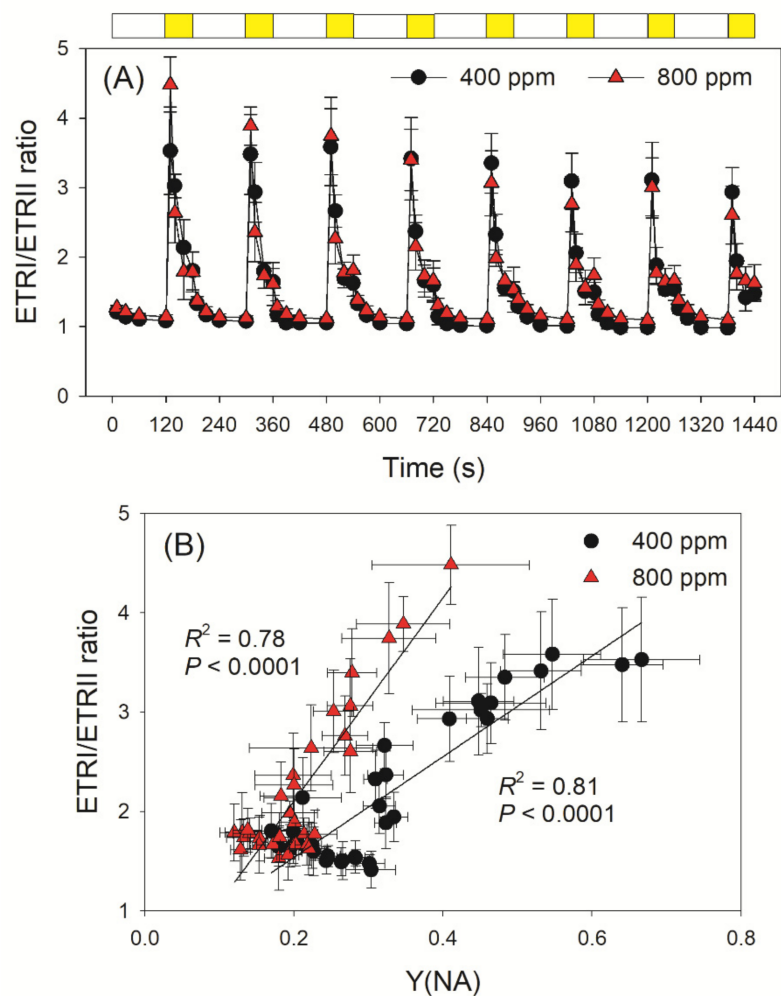


**Figure 5.** Changes in ETRI/ETR II ratio under fluctuating light and its relationship to Y(NA) in high-light phases. (A) Change in the ratio of ETRI/ETR II during fluctuating light alternating between 59 and 1809  $\mu\text{mol photons m}^{-2} \text{s}^{-1}$  in Arabidopsis leaves measured in 400 and 800 ppm CO<sub>2</sub>; (B) Relationship between the ETRI/ETR II ratio and Y(NA) during the high light phase of fluctuating light treatments. Data are shown as means  $\pm$  SD (n = 5). White bars indicate low light (59  $\mu\text{mol photons m}^{-2} \text{s}^{-1}$ ); yellow bars indicate high light (1809  $\mu\text{mol photons m}^{-2} \text{s}^{-1}$ ).

PSI redox state under FL is determined by donor- and acceptor-side regulation. To further explore the effect of elevated atmospheric CO<sub>2</sub> on PSI redox state under FL, we examined the relationships between NPQ, Y(ND) and Y(NA) after transition from LL to HL for 10 s. Irrespective of the CO<sub>2</sub> concentration, NPQ<sub>10s</sub> was positively correlated to Y(ND)<sub>10s</sub> but was negatively correlated to Y(NA)<sub>10s</sub> (Figure 6). These results indicated that an increase in  $\Delta\text{pH}$  facilitates the oxidation of PSI and thus prevents an over-reduction of PSI. Meanwhile, the same value of NPQ<sub>10s</sub> was accompanied by a higher Y(ND)<sub>10s</sub> and a lower Y(NA)<sub>10s</sub> in 800 ppm CO<sub>2</sub> (Figure 6), suggesting that elevated atmospheric CO<sub>2</sub> affects the PSI redox state under FL mainly at acceptor side rather than at donor side.

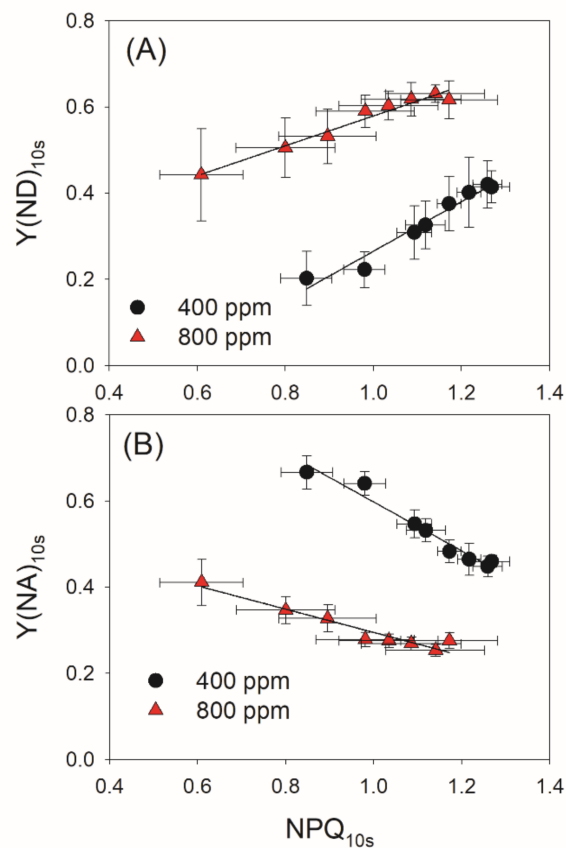


**Figure 6.** Relationships between NPQ and PSI redox state after transition from low to high light for 10 s in the eight cycles of low/high light. (A) Relationship between NPQ<sub>10s</sub> and Y(ND)<sub>10s</sub>; (B) Relationship between NPQ<sub>10s</sub> and Y(NA)<sub>10s</sub>. Data are prepared by combining the different time points of Figures 3 and 4.

### 3.3. Elevated Atmospheric CO<sub>2</sub> Concentrations Mitigates PSI Photoinhibition under FL

After FL treatment, we measured  $F_v/F_m$  and  $P_m$  to evaluate PSI and PSII photoinhibition. Irrespective of the CO<sub>2</sub> concentration, PSI photoinhibition under FL was more evident than that of PSII (Figure 7A). In addition, elevated atmospheric CO<sub>2</sub> did not affect the extent of PSII photoinhibition but alleviated PSI photoinhibition (Figure 7A). After FL treatment,  $P_m$  decreased by 25% and 16% in 400 and 800 ppm CO<sub>2</sub>, respectively, relative to  $P_m$  values before FL (Figure 7A). The stronger PSI photoinhibition seen in 400 ppm CO<sub>2</sub> was mainly caused by the higher Y(NA) within the first 20 s after the transition from LL to HL (Figure 7B). A higher Y(NA) represents a stronger over-reduction of PSI, which leads to the generation of ROS in PSI and thus causes PSI photoinhibition.

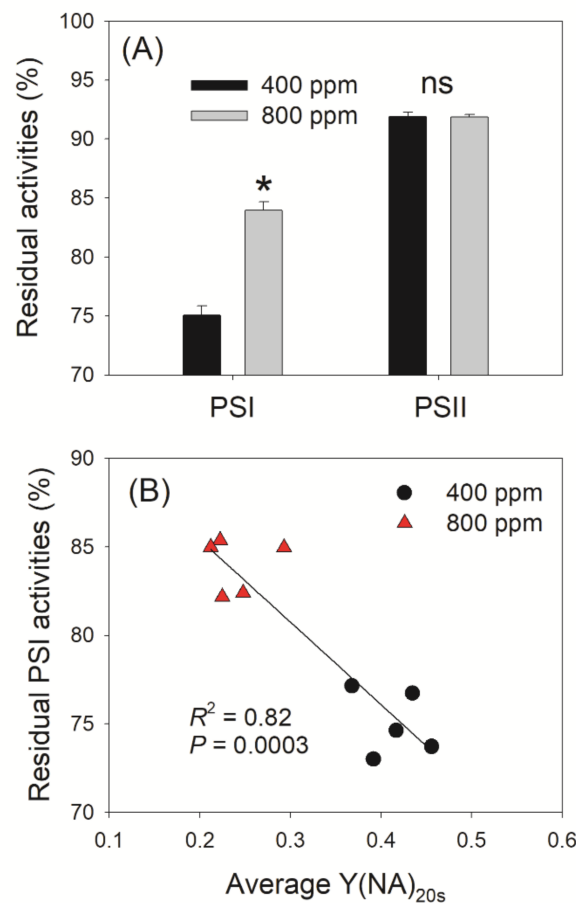


**Figure 7.** Effect of elevated CO<sub>2</sub> concentration of photoinhibition under fluctuating light and its relationship to redox state of PSI. **(A)** Changes in  $P_m$  and  $F_v/F_m$  after exposure to fluctuating light for 24 min.  $F_v/F_m$  and  $P_m$  represent photosystem PSII and PSI activity, respectively; **(B)** Relationship between residual PSI activity and the mean value of  $Y(NA)_{20s}$  after transition to high light for 20 s ( $Y(NA)_{20s}$ ). Data are shown as means  $\pm$  SD (n = 5). Asterisk indicates a significant different between 400 and 800 ppm.

#### 4. Discussion

Plants usually undergo FL under natural field conditions [7,14]. Following a sudden increase in illumination, the corresponding rapid rise in light absorption and electron flow from PSII cannot be immediately consumed by the CO<sub>2</sub> fixation machinery, which displays much slower kinetics than ETRII [9,31,32,46]. As a result, excited states in PSI cannot be immediately transported to NADP<sup>+</sup>, leading to the over-reduction of PSI electron carriers and inducing the production of ROS within PSI [15,16,47]. However, ROS cannot be immediately scavenged by the antioxidant system, thereby causing photodamage to PSI [17]. A higher atmospheric CO<sub>2</sub> concentration, such as that resulting from industrial activities and behind the global climate change crisis, will facilitate CO<sub>2</sub> fixation after transition from LL to HL [13]. Therefore, we hypothesized that elevated atmospheric CO<sub>2</sub> might mitigate PSI photoinhibition under FL.

To test this hypothesis, we measured the chlorophyll fluorescence and P700 signals under FL conditions in 400 and 800 ppm CO<sub>2</sub>. We documented that an elevated CO<sub>2</sub> concentration significantly affected the redox state of PSI after any increase in light intensity. Upon transition from darkness to high light (1809  $\mu\text{mol photons m}^{-2} \text{s}^{-1}$ ) for 20 s, P700 was highly reduced in 400 ppm CO<sub>2</sub> but was re-oxidized in 800 ppm CO<sub>2</sub> (Figure 1). Similarly, after transition from darkness to 272  $\mu\text{mol photons m}^{-2} \text{s}^{-1}$  for 30 s, leaves showed a low value of  $Y(ND)$  in 400 ppm CO<sub>2</sub>, causing PSI to be over-reduced (Figure 2). By contrast, over the same time frame, leaves showed a high  $Y(ND)$  value in 800 ppm CO<sub>2</sub>, indicating

that the higher CO<sub>2</sub> concentration prevents PSI over-reduction (Figure 2). Furthermore, after transition from LL to HL for 20 s, the over-reduction of PSI was alleviated by the elevated CO<sub>2</sub> concentration (Figure 3). When P700 is highly oxidized, the probability of electron donation from P700 to O<sub>2</sub> is suppressed. Therefore, oxidation of P700 can prevent the production of ROS within PSI and thus protect PSI against excess light energy [48]. Consistently, the extent of PSI photoinhibition under FL was mainly determined by the over-reduction of PSI within the first 20 s after exposure to HL (Figure 7). Therefore, the elevated atmospheric CO<sub>2</sub> concentration significantly contributed to preventing PSI photoinhibition under FL in *Arabidopsis* leaves.

PSI photoinhibition occurs only when electrons transferred to PSI cannot be immediately transported to downstream electron acceptors [10,49,50]. The PSI redox state under FL can be regulated at the donor and acceptor sides. On the donor-side regulation, the ΔpH-dependent photosynthetic control at the Cyt *b*<sub>6</sub>/*f* complex slows electron transfer from PSII to PSI, thus decreasing the excitation pressure on PSI [22,24,33,51]. Upon a sudden transition from LL to HL, the transient stimulation of CEF facilitates the rapid formation of a ΔpH, which prevents uncontrolled photoinhibition of PSI under FL conditions [18,29,47]. The impairment of CEF strongly accelerates PSI photoinhibition under FL, leading to the death of *pgr5* seedlings under FL [16,18,23]. In agreement, we also observed the transient stimulation of CEF upon transition from LL to HL in both 400 and 800 ppm CO<sub>2</sub> (Figure 6), indicating that CEF plays a major role in photoprotection for PSI under FL irrespective of CO<sub>2</sub> concentration. In addition, either PSII photoinhibition or minimizing the activity of the oxygen-evolving complex can restrict electron flow to PSI and thus protect PSI at donor side [49,52,53]. Indeed, minimizing the activity of the oxygen-evolving complex can rescue the phenotype of *pgr5* plants under FL [52]. In this study, we observed that NPQ induction under FL is not influenced by an elevated CO<sub>2</sub> concentration (Figure 4B), suggesting that higher CO<sub>2</sub> levels hardly affected the formation of ΔpH under FL. Furthermore, the CEF stimulation under FL remained unchanged by the CO<sub>2</sub> concentrations employed here (Figure 5). Therefore, the effect of elevated CO<sub>2</sub> on the redox state of PSI under FL cannot be explained by regulation on the donor side. As shown in Figure 6, the relationships between NPQ, Y(ND) and Y(NA) under FL were altered by the elevated atmospheric CO<sub>2</sub> concentration, suggesting that elevated atmospheric CO<sub>2</sub> concentration influenced the PSI redox state under FL at the acceptor side rather than at the donor side.

The acceptor-side regulation of PSI is mainly attributed to electron transport from PSI to downstream electron acceptors. In photosynthetic organisms, three pathways are responsible for the regulation of PSI on the acceptor side [24,43]: (1) electron transport from PSI to NADP<sup>+</sup>; (2) the Mehler reaction (water–water cycle); (3) O<sub>2</sub> photoreduction mediated by flavodiiron proteins (Flvs). Flvs are present in photosynthetic organisms ranging from cyanobacteria to gymnosperms but appear to have been lost in angiosperms during evolution [15,43,54]. In addition, the activity of the water–water cycle in angiosperms is species-dependent [30,45,46]. In *Arabidopsis* leaves, the P700 redox kinetics upon transition from darkness to light indicated that the activity of the water–water cycle is negligible (Figure 1). Therefore, the rapid oxidation of PSI under FL under elevated CO<sub>2</sub> is likely to be attributed to accelerated electron transfer from PSI to NADP<sup>+</sup>. The electron transfer from PSI to NADP<sup>+</sup> is largely affected by the NADP<sup>+</sup>/NADPH ratio. At elevated CO<sub>2</sub> concentrations, CO<sub>2</sub> fixation under FL increases [38], raising the rate of NADPH consumption. Under such conditions, the NADP<sup>+</sup>/NADPH ratio increases, facilitating electron transfer from PSI to NADP<sup>+</sup> and thus alleviating the over-reduction of PSI electron carriers. Therefore, elevated CO<sub>2</sub> affects the PSI redox state under FL through the acceptor-side regulation.

Improving photosynthesis under FL is a critical and timely target for crop improvement under field conditions [9,13,14,55]. Maintaining high photosynthetic rates requires the avoidance of photoinhibition [6,56–58]. However, FL-induced photoinhibition of PSI can significantly affect CO<sub>2</sub> assimilation [5]. Therefore, diminishing the extent of PSI photoinhibition under FL is an effective way to improve photosynthesis under natural

FL. Raising CO<sub>2</sub> concentrations can significantly boost crop yields and is thought to be attributed to enhanced photosynthetic rates [36,39]. Furthermore, we discovered here that elevated CO<sub>2</sub> can significantly alter the PSI redox state under FL and thus mitigate FL-induced photoinhibition of PSI, which in turn safeguards high rates of photosynthesis. Therefore, in addition to dark reactions, elevated CO<sub>2</sub> concentrations can have large effects on thylakoid reactions under FL conditions.

**Author Contributions:** Conceptualization, W.H. and S.-B.Z.; methodology, W.H. and S.-L.T.; validation, W.H. and S.-B.Z.; formal analysis, S.-L.T.; investigation, S.-L.T.; resources, X.H. and W.-Q.L.; data curation, S.-L.T. and W.H.; writing—original draft preparation, W.H.; writing—review and editing, S.-B.Z.; supervision, S.-B.Z.; project administration, W.H.; funding acquisition, W.H. and S.-B.Z. All authors have read and agreed to the published version of the manuscript.

**Funding:** This work was supported by the National Natural Science Foundation of China (Grant 31971412), Project for Construction of International Flower Technology Innovation Center and Achievement Industrialization (2019ZG006) and the Project for Innovation Team of Yunnan Province.

**Institutional Review Board Statement:** Not applicable.

**Informed Consent Statement:** Not applicable.

**Data Availability Statement:** Not applicable.

**Conflicts of Interest:** The authors declare that they have no conflict of interest.

## References

1. Acevedo-Siaca, L.G.; Coe, R.; Wang, Y.; Kromdijk, J.; Quick, W.P.; Long, S.P. Variation in photosynthetic induction between rice accessions and its potential for improving productivity. *New Phytol.* **2020**, *227*, 1097–1108. [[CrossRef](#)]
2. Allahverdiyeva, Y.; Suorsa, M.; Tikkanen, M.; Aro, E.M. Photoprotection of photosystems in fluctuating light intensities. *J. Exp. Bot.* **2015**, *66*, 2427–2436. [[CrossRef](#)] [[PubMed](#)]
3. Ananyev, G.; Kolber, Z.S.; Klimov, D.; Falkowski, P.G.; Berry, J.A.; Rascher, U.; Martin, R.; Osmond, B. Remote sensing of heterogeneity in photosynthetic efficiency, electron transport and dissipation of excess light in *Populus deltoides* stands under ambient and elevated CO<sub>2</sub> concentrations, and in a tropical forest canopy, using a new laser-induced fluoresc. *Glob. Chang. Biol.* **2005**, *11*, 1195–1206. [[CrossRef](#)]
4. Armbruster, U.; Correa Galvis, V.; Kunz, H.H.; Strand, D.D. The regulation of the chloroplast proton motive force plays a key role for photosynthesis in fluctuating light. *Curr. Opin. Plant. Biol.* **2017**, *37*, 56–62. [[CrossRef](#)]
5. Brestic, M.; Zivcak, M.; Kunderlikova, K.; Allakhverdiev, S.I. High temperature specifically affects the photoprotective responses of chlorophyll b-deficient wheat mutant lines. *Photosynth. Res.* **2016**, *130*, 251–266. [[CrossRef](#)]
6. Brestic, M.; Zivcak, M.; Kunderlikova, K.; Sytar, O.; Shao, H.; Kalaji, H.M.; Allakhverdiev, S.I. Low PSI content limits the photoprotection of PSI and PSII in early growth stages of chlorophyll b-deficient wheat mutant lines. *Photosynth. Res.* **2015**, *125*, 151–166. [[CrossRef](#)]
7. De Souza, A.P.; Wang, Y.; Orr, D.J.; Carmo-Silva, E.; Long, S.P. Photosynthesis across African cassava germplasm is limited by Rubisco and mesophyll conductance at steady state, but by stomatal conductance in fluctuating light. *New Phytol.* **2020**, *225*, 2498–2512. [[CrossRef](#)]
8. Ferroni, L.; Živčák, M.; Sytar, O.; Kovár, M.; Watanabe, N.; Pancaldi, S.; Baldissarotto, C.; Brestič, M. Chlorophyll-depleted wheat mutants are disturbed in photosynthetic electron flow regulation but can retain an acclimation ability to a fluctuating light regime. *Environ. Exp. Bot.* **2020**, *178*, 104156. [[CrossRef](#)]
9. Gerotto, C.; Alboresi, A.; Meneghesso, A.; Jokel, M.; Suorsa, M.; Aro, E.-M.; Morosinotto, T. Flavodiiron proteins act as safety valve for electrons in *Physcomitrella patens*. *Proc. Natl. Acad. Sci. USA* **2016**, *113*, 12322–12327. [[CrossRef](#)] [[PubMed](#)]
10. Hendrickson, L.; Furbank, R.T.; Chow, W.S. A simple alternative approach to assessing the fate of absorbed light energy using chlorophyll fluorescence. *Photosynth. Res.* **2004**, *82*, 73–81. [[CrossRef](#)] [[PubMed](#)]
11. Huang, W.; Yang, Y.-J.; Zhang, S.-B. Photoinhibition of photosystem I under fluctuating light is linked to the insufficient ΔpH upon a sudden transition from low to high light. *Environ. Exp. Bot.* **2019**, *160*, 112–119. [[CrossRef](#)]
12. Huang, W.; Yang, Y.-J.; Zhang, S.-B. The role of water-water cycle in regulating the redox state of photosystem I under fluctuating light. *Biochim. Biophys. Acta Bioenerg.* **2019**, *1860*, 383–390. [[CrossRef](#)] [[PubMed](#)]
13. Huang, W.; Zhang, S.-B.; Liu, T. Moderate photoinhibition of photosystem II significantly affects linear electron flow in the shade-demanding plant *Panax notoginseng*. *Front. Plant. Sci.* **2018**, *9*, 637. [[CrossRef](#)] [[PubMed](#)]
14. Ilík, P.; Pavlovič, A.; Kouřil, R.; Alboresi, A.; Morosinotto, T.; Allahverdiyeva, Y.; Aro, E.M.; Yamamoto, H.; Shikanai, T. Alternative electron transport mediated by flavodiiron proteins is operational in organisms from cyanobacteria up to gymnosperms. *New Phytol.* **2017**, *214*, 967–972. [[CrossRef](#)]

15. Jokel, M.; Johnson, X.; Peltier, G.; Aro, E.M.; Allahverdiyeva, Y. Hunting the main player enabling *Chlamydomonas reinhardtii* growth under fluctuating light. *Plant., J.* **2018**, *94*, 822–835. [[CrossRef](#)]
16. Kimura, H.; Hashimoto-Sugimoto, M.; Iba, K.; Terashima, I.; Yamori, W. Improved stomatal opening enhances photosynthetic rate and biomass production in fluctuating light. *J. Exp. Bot.* **2020**, *71*, 2339–2350. [[CrossRef](#)]
17. Kono, M.; Noguchi, K.; Terashima, I. Roles of the cyclic electron flow around PSI (CEF-PSI) and O<sub>2</sub>-dependent alternative pathways in regulation of the photosynthetic electron flow in short-term fluctuating light in *Arabidopsis thaliana*. *Plant. Cell Physiol.* **2014**, *55*, 990–1004. [[CrossRef](#)]
18. Kramer, D.M.; Johnson, G.; Kiirats, O.; Edwards, G.E. New fluorescence parameters for the determination of Q A redox state and excitation energy fluxes. *Photosynth. Res.* **2004**, *79*, 209–218. [[CrossRef](#)]
19. Kreslavski, V.D.; Strokina, V.V.; Pashkovskiy, P.P.; Balakhnina, T.I.; Voloshin, R.A.; Alwasel, S.; Kosobryukhov, A.A.; Allakhverdiev, S.I. Deficiencies in phytochromes A and B and cryptochrome 1 affect the resistance of the photosynthetic apparatus to high-intensity light in *Solanum lycopersicum*. *J. Photochem. Photobiol. B Biol.* **2020**, *210*, 111976. [[CrossRef](#)] [[PubMed](#)]
20. Munekage, Y.N.; Genty, B.; Peltier, G. Effect of PGR5 impairment on photosynthesis and growth in *Arabidopsis thaliana*. *Plant. Cell Physiol.* **2008**, *49*, 1688–1698. [[CrossRef](#)]
21. Nakano, H.; Yamamoto, H.; Shikanai, T. Contribution of NDH-dependent cyclic electron transport around photosystem I to the generation of proton motive force in the weak mutant allele of *pgr5*. *Biochim. Biophys. Acta Bioenerg.* **2019**, *1860*, 369–374. [[CrossRef](#)]
22. Nawrocki, W.J.; Bailleul, B.; Cardol, P.; Rappaport, F.; Wollman, F.A.; Joliot, P. Maximal cyclic electron flow rate is independent of PGRL1 in *Chlamydomonas*. *Biochim. Biophys. Acta Bioenerg.* **2019**, *1860*, 425–432. [[CrossRef](#)] [[PubMed](#)]
23. Nawrocki, W.J.; Bailleul, B.; Picot, D.; Cardol, P.; Rappaport, F.; Wollman, F.A.; Joliot, P. The mechanism of cyclic electron flow. *Biochim. Biophys. Acta Bioenerg.* **2019**, *1860*, 433–438. [[CrossRef](#)] [[PubMed](#)]
24. Pearcy, R.W. Sunflecks and photosynthesis in plant canopies. *Annu. Rev. Plant. Physiol. Plant. Mol. Biol.* **1990**, *41*, 421–453. [[CrossRef](#)]
25. Qiao, M.-Y.; Zhang, Y.-J.; Liu, L.-A.; Shi, L.; Ma, Q.-H.; Chow, W.S.; Jiang, C.-D. Do rapid photosynthetic responses protect maize leaves against photoinhibition under fluctuating light? *Photosynth. Res.* **2020**. [[CrossRef](#)]
26. Sakoda, K.; Yamori, W.; Shimada, T.; Sugano, S.S.; Hara-Nishimura, I.; Tanaka, Y. Higher stomatal density improves photosynthetic induction and biomass production in *Arabidopsis* under fluctuating light. *Front. Plant. Sci.* **2020**, *11*, 1308. [[CrossRef](#)]
27. Salter, W.T.; Merchant, A.M.; Richards, R.A.; Trethowan, R.; Buckley, T.N. Rate of photosynthetic induction in fluctuating light varies widely among genotypes of wheat. *J. Exp. Bot.* **2019**, *70*, 2787–2796. [[CrossRef](#)]
28. Schreiber, U.; Klughammer, C. Non-photochemical fluorescence quenching and quantum yields in PS I and PS II: Analysis of heat-induced limitations using Maxi-Imaging-PAM and Dual-PAM-100. *PAM Appl. Notes* **2008**, *1*, 15–18. [[CrossRef](#)]
29. Shikanai, T.; Yamamoto, H. Contribution of cyclic and pseudo-cyclic electron transport to the formation of proton motive force in chloroplasts. *Mol. Plant.* **2017**, *10*, 20–29. [[CrossRef](#)]
30. Shimakawa, G.; Miyake, C. What quantity of photosystem I is optimum for safe photosynthesis? *Plant. Physiol.* **2019**, *179*, 1479–1485. [[CrossRef](#)]
31. Slattery, R.A.; Walker, B.J.; Weber, A.P.M.; Ort, D.R. The impacts of fluctuating light on crop performance. *Plant. Physiol.* **2018**, *176*, 990–1003. [[CrossRef](#)] [[PubMed](#)]
32. Sun, H.; Yang, Y.-J.; Huang, W. The water-water cycle is more effective in regulating redox state of photosystem I under fluctuating light than cyclic electron transport. *Biochim. Biophys. Acta Bioenerg.* **2020**, *1861*, 148235. [[CrossRef](#)] [[PubMed](#)]
33. Sun, H.; Zhang, S.-B.; Liu, T.; Huang, W. Decreased photosystem II activity facilitates acclimation to fluctuating light in the understory plant *Paris polyphylla*. *Biochim. Biophys. Acta Bioenerg.* **2020**, *1861*, 148135. [[CrossRef](#)] [[PubMed](#)]
34. Suorsa, M.; Jarvi, S.; Grieco, M.; Nurmi, M.; Pietrzykowska, M.; Rantala, M.; Kangasjarvi, S.; Paakkari, V.; Tikkanen, M.; Jansson, S.; et al. PROTON GRADIENT REGULATION5 is essential for proper acclimation of *Arabidopsis* photosystem I to naturally and artificially fluctuating light conditions. *Plant. Cell* **2012**, *24*, 2934–2948. [[CrossRef](#)]
35. Suorsa, M.; Rossi, F.; Tadini, L.; Labs, M.; Colombo, M.; Jahns, P.; Kater, M.M.; Leister, D.; Finazzi, G.; Aro, E.-M.; et al. PGR5-PGRL1-dependent cyclic electron transport modulates linear electron transport rate in *Arabidopsis thaliana*. *Mol. Plant.* **2016**, *9*, 271–288. [[CrossRef](#)] [[PubMed](#)]
36. Takagi, D.; Amako, K.; Hashiguchi, M.; Fukaki, H.; Ishizaki, K.; Goh, T.; Fukao, Y.; Sano, R.; Kurata, T.; Demura, T.; et al. Chloroplastic ATP synthase builds up a proton motive force preventing production of reactive oxygen species in photosystem I. *Plant. J.* **2017**, *91*, 306–324. [[CrossRef](#)] [[PubMed](#)]
37. Takagi, D.; Ishizaki, K.; Hanawa, H.; Mabuchi, T.; Shimakawa, G.; Yamamoto, H.; Miyake, C. Diversity of strategies for escaping reactive oxygen species production within photosystem I among land plants: P700 oxidation system is prerequisite for alleviating photoinhibition in photosystem I. *Physiol. Plant.* **2017**, *161*, 56–74. [[CrossRef](#)] [[PubMed](#)]
38. Takagi, D.; Takumi, S.; Hashiguchi, M.; Sejima, T.; Miyake, C. Superoxide and singlet oxygen produced within the thylakoid membranes both cause photosystem I photoinhibition. *Plant. Physiol.* **2016**, *171*, 1626–1634. [[CrossRef](#)]
39. Tan, S.-L.; Huang, J.-L.; Zhang, F.-P.; Zhang, S.-B.; Huang, W. Photosystem I photoinhibition induced by fluctuating light depends on background low light irradiance. *Environ. Exp. Bot.* **2021**, *181*, 104298. [[CrossRef](#)]
40. Tan, S.-L.; Liu, T.; Zhang, S.-B.; Huang, W. Balancing light use efficiency and photoprotection in tobacco leaves grown at different light regimes. *Environ. Exp. Bot.* **2020**, *175*, 104046. [[CrossRef](#)]

41. Tan, S.-L.; Yang, Y.-J.; Huang, W. Moderate heat stress accelerates photoinhibition of photosystem I under fluctuating light in tobacco young leaves. *Photosynth. Res.* **2020**, *144*, 373–382. [[CrossRef](#)]
42. Tan, S.-L.; Yang, Y.-J.; Liu, T.; Zhang, S.-B.; Huang, W. Responses of photosystem I compared with photosystem II to combination of heat stress and fluctuating light in tobacco leaves. *Plant. Sci.* **2020**, *292*, 110371. [[CrossRef](#)]
43. Tikkanen, M.; Aro, E.M. Integrative regulatory network of plant thylakoid energy transduction. *Trends Plant. Sci.* **2014**, *19*, 10–17. [[CrossRef](#)] [[PubMed](#)]
44. Tikkanen, M.; Grieco, M.; Nurmi, M.; Rantala, M.; Suorsa, M.; Aro, E.-M. Regulation of the photosynthetic apparatus under fluctuating growth light. *Philos. Trans. R. Soc. B Biol. Sci.* **2012**, *367*, 3486–3493. [[CrossRef](#)]
45. Tikkanen, M.; Mekala, N.R.; Aro, E.-M. Photosystem II photoinhibition-repair cycle protects Photosystem I from irreversible damage. *Biochim. Biophys. Acta Bioenerg.* **2014**, *1837*, 210–215. [[CrossRef](#)] [[PubMed](#)]
46. Wada, S.; Yamamoto, H.; Suzuki, Y.; Yamori, W.; Shikanai, T.; Makino, A. Flavodiiron protein substitutes for cyclic electron flow without competing CO<sub>2</sub> assimilation in rice. *Plant. Physiol.* **2018**, *176*, 1509–1518. [[CrossRef](#)] [[PubMed](#)]
47. Walker, B.J.; Strand, D.D.; Kramer, D.M.; Cousins, A.B. The response of cyclic electron flow around photosystem I to changes in photorespiration and nitrate assimilation. *Plant. Physiol.* **2014**, *165*, 453–462. [[CrossRef](#)] [[PubMed](#)]
48. Yamamoto, H.; Shikanai, T. PGR5-dependent cyclic electron flow protects photosystem I under fluctuating light at donor and acceptor sides. *Plant. Physiol.* **2019**, *179*, 588–600. [[CrossRef](#)] [[PubMed](#)]
49. Yamamoto, H.; Takahashi, S.; Badger, M.R.; Shikanai, T. Artificial remodelling of alternative electron flow by flavodiiron proteins in Arabidopsis. *Nat. Plants* **2016**, *2*, 16012. [[CrossRef](#)] [[PubMed](#)]
50. Yamori, W.; Kusumi, K.; Iba, K.; Terashima, I. Increased stomatal conductance induces rapid changes to photosynthetic rate in response to naturally fluctuating light conditions in rice. *Plant. Cell Environ.* **2020**, *43*, 1230–1240. [[CrossRef](#)] [[PubMed](#)]
51. Yamori, W.; Makino, A.; Shikanai, T. A physiological role of cyclic electron transport around photosystem I in sustaining photosynthesis under fluctuating light in rice. *Sci. Rep.* **2016**, *6*, 20147. [[CrossRef](#)] [[PubMed](#)]
52. Yang, Y.-J.; Ding, X.-X.; Huang, W. Stimulation of cyclic electron flow around photosystem I upon a sudden transition from low to high light in two angiosperms Arabidopsis thaliana and Bletilla striata. *Plant. Sci.* **2019**, *287*, 110166. [[CrossRef](#)]
53. Yang, Y.-J.; Tan, S.-L.; Huang, J.-L.; Zhang, S.-B.; Huang, W. The water-water cycle facilitates photosynthetic regulation under fluctuating light in the epiphytic orchid Dendrobium officinale. *Environ. Exp. Bot.* **2020**, *180*, 104238. [[CrossRef](#)]
54. Yang, Y.-J.; Zhang, S.-B.; Huang, W. Photosynthetic regulation under fluctuating light in young and mature leaves of the CAM plant Bryophyllum pinnatum. *Biochim. Biophys. Acta Bioenerg.* **2019**, *1860*, 469–477. [[CrossRef](#)] [[PubMed](#)]
55. Yang, Y.-J.; Zhang, S.-B.; Wang, J.-H.; Huang, W. Photosynthetic regulation under fluctuating light in field-grown Cerasus cerasoides: A comparison of young and mature leaves. *Biochim. Biophys. Acta Bioenerg.* **2019**, *1860*, 148073. [[CrossRef](#)] [[PubMed](#)]
56. Zhang, D.; Xu, J.; Bao, M.; Yan, D.; Beer, S.; Beardall, J.; Gao, K. Elevated CO<sub>2</sub> concentration alleviates UVR-induced inhibition of photosynthetic light reactions and growth in an intertidal red macroalga. *J. Photochem. Photobiol. B Biol.* **2020**, *213*, 112074. [[CrossRef](#)]
57. Zivcak, M.; Brestic, M.; Kunderlikova, K.; Sytar, O.; Allakhverdiev, S.I. Repetitive light pulse-induced photoinhibition of photosystem I severely affects CO<sub>2</sub> assimilation and photoprotection in wheat leaves. *Photosynth. Res.* **2015**, *126*, 449–463. [[CrossRef](#)]
58. Zlobin, I.E.; Kartashov, A.V.; Pashkovskiy, P.P.; Ivanov, Y.V.; Kreslavski, V.D.; Kuznetsov, V.V. Comparative photosynthetic responses of Norway spruce and Scots pine seedlings to prolonged water deficiency. *J. Photochem. Photobiol. B Biol.* **2019**, *201*, 111659. [[CrossRef](#)]